Synthetic and Systems Biotechnology 10 (2025) 555–563

Contents lists available at ScienceDirect

Synthetic and Systems Biotechnology

journal homepage: www.keaipublishing.com/en/journals/synthetic-and-systems-biotechnology

Original Research Article

Development of CRISPR-Cas9-based genome editing tools for non-model microorganism *Erwinia persicina*

Tingfeng Cheng [a,b], Xinyan Cao [a,c], Yuchen Wang [a,d], Lei Zhao [a,b,c,*]

[a] State Key Laboratory of Engineering Biology for Low-Carbon Manufacturing, Tianjin Institute of Industrial Biotechnology, Chinese Academy of Sciences, Tianjin, 300308, PR China
[b] University of Chinese Academy of Sciences, Beijing, 100049, PR China
[c] National Center of Technology Innovation for Synthetic Biology, Tianjin, 300308, PR China
[d] College of Biological Sciences, China Agricultural University, Beijing, 100091, PR China

ARTICLE INFO

Keywords:
Erwinia persicina
CRISPR-Cas9
Genome editing
Non-model microorganism
Shinorine

ABSTRACT

Erwinia persicina is a bacterium that has been known to produce secondary metabolites, such as andrimid, pink pigment, and exopolysaccharides, and to infect more than twenty plant species. However, traditional gene manipulation methods have been hindered by the inefficient of suicide plasmid-mediated genome editing. In this study, we describe the successful application of the CRISPR-Cas9 system in *E. persicina*. Efficient genome editing was achieved by substituting the native gRNA promoter with J23119 in a single-plasmid system (pRed_Cas9_Δ*poxB*) and optimizing the gRNA design. The use of double gRNAs led to the deletion of a 42 kb genomic fragment, and the incorporation of a *sacB* screening marker facilitated iterative knockouts. Additionally, a 22 kb plasmid containing a self-resistance gene was conjugally transferred into *E. persicina*, resulting in the insertion of a 6.4 kb fragment with 100 % efficiency. Furthermore, we demonstrated the expression of shinorine, an anti-UV compound, within the *E. persicina* chassis. This study establishes *E. persicina* as a promising chassis for synthetic biology and provides a model for gene-editing systems in non-model microorganisms.

1. Introduction

Erwinia persicina is a non-model, rod-shaped bacterium belonging to the family Enterobacteriaceae [1]. It exhibits a broad spectrum of substrate utilization, encompassing a wide range of carbon compounds and nitrogen sources [2]. *E. persicina* is commonly associated with plants and produces a variety of secondary metabolites, making it a promising chassis strain for the expression of diverse compounds. Recent studies have demonstrated that *E. persicina* exhibits both phosphorus-solubilizing and biocontrol capabilities, which significantly enhance plant phosphate concentrations and mitigate the severity of Fusarium head blight (FHB) in wheat [3,4]. Furthermore, the exopolysaccharides and pink pigment produced by *E. persicina* Cp2 have been shown to promote alfalfa growth under NaCl stress and exhibit antifungal properties [5,6]. *E. persicina* BST187 has been shown to demonstrate potent inhibitory activity against pathogenic bacteria through the production of andrimid, which inhibits bacterial acetyl-CoA carboxylase [7]. Additionally, *E. persicina* EUS78 has also shown significant potential as a biological control agent in the food industry, specifically against *Salmonella enterica* contamination in sprouts [8].

The genus *Erwinia* is predominantly comprised of plant pathogenic species, with *E. amylovora* being a prominent example that has been identified as the causative agent of fire blight disease in ornamentals, fruit trees, and shrubs [9]. As an opportunistic pathogen, *E. persicina* poses a substantial threat to agricultural production by causing pink-pigmented soft rot in various plant hosts, including garlic (*Allium sativum*), onion (*Allium cepa*), celery (*Apium graveolens*), and parsley (*Petroselinum crispum*) [10–13]. In addition to vegetables, *E. persicina* also infects many economically important crops, including legumes and herbaceous plants [14,15]. The advent of efficient genome editing methodologies holds considerable promise in enhancing our comprehension of the pathogenic mechanisms of *E. persicina* and for developing strategies for effective disease control by investigating its interactions with plants and other microorganisms. The conventional gene

Peer review under the responsibility of Editorial Board of Synthetic and Systems Biotechnology.
* Corresponding author. State Key Laboratory of Engineering Biology for Low-Carbon Manufacturing, Tianjin Institute of Industrial Biotechnology, Chinese Academy of Sciences, Tianjin, 300308, PR China.
E-mail address: zhaol@tib.cas.cn (L. Zhao).

https://doi.org/10.1016/j.synbio.2025.02.006
Received 20 November 2024; Received in revised form 20 January 2025; Accepted 12 February 2025
Available online 18 February 2025
2405-805X/© 2025 The Authors. Publishing services by Elsevier B.V. on behalf of KeAi Communications Co. Ltd. This is an open access article under the CC BY-NC-ND license (http://creativecommons.org/licenses/by-nc-nd/4.0/).

manipulation method employed in *E. persicina* relies on a suicide plasmid-mediated genome editing system. However, this approach is both time-consuming (requiring approximately 6–10 days to modify a chromosomal locus) and inefficient (with knockout efficiency varying depending on the target gene and editing efficiency ranging from 10 % to 80 %) [16].

The clustered regularly interspaced short palindromic repeats (CRISPR)/CRISPR-associated (Cas) systems have emerged as powerful tools for precise microbial genome editing. In this system, Cas proteins generate double-stranded DNA breaks (DSBs), which subsequently activate homologous recombination (HR), the predominant mechanism for repairing DSBs in bacteria [17]. Despite the prevalence of endogenous CRISPR systems within the *Erwinia* genus, their application remains restricted due to the absence of non-homologous end joining (NHEJ) [18,19]. The CRISPR-Cas9-based cytosine base editing system has been reported in *E. amylovora* and has demonstrated high-efficiency for both single and multiple gene editing. However, it should be noted that even within the same species, the CRISPR-Cas plasmids is not universally applicable. For instance, the pCas/pTargetF two-plasmid system has been widely used in *Escherichia coli* K-12 strain MG1655 but has failed in *Es. coli* BL21 due to excessive leakage expression of gRNA-pMB1 on the pCas plasmid [20]. Genome editing can be successfully performed in BL21 using a modified pCas/pTarget system (pEcCas/pEcgRNA) [21]. Furthermore, it has been demonstrated that not all the tools developed from CRISPR-Cas systems are functional in non-model microorganisms. For instance, the CRISPR-Cas9 plasmids exert a substantial metabolic burden on strains, leading to toxic effects and reduced transfection efficiency [22]. Moreover, non-model microorganisms most possess diverse restriction-modification (R-M) systems, necessitating the development of effective DNA delivery methods for these bacteria [23]. Conjugative transfer, initiated by the contact between donor and recipient strains, is driven by plasmids within the donor strains, ensuring the integrity of plasmid DNA in the donor strains, making conjugative transfer a promising method for large DNA transfer. This method has been successfully applied in suicide plasmid-mediated genome editing in *E. persicina* [16,24].

Non-model microorganisms have demonstrated significant potential for applications in research, medicine, environmental management, and biomanufacturing. For instance, L-asparaginase has been shown to play a critical role in the treatment of acute lymphoblastic leukemia (ALL). Erwinase®, a commercial form of L-asparaginase derived from *E. chrysanthemi*, is the only available asparaginase therapy for ALL patients with hypersensitivity to *Es. coli*-derived asparaginases. However, its use is limited by issues regarding its availability [25]. JZP-458, a recombinant form of *Erwinia* asparaginase derived from a novel *Pseudomonas fluorescens* expression platform, was approved by the FDA in 2021. This approval has facilitated a more stable and efficient production process, thereby alleviating supply chain challenges [26]. Furthermore, *E. persicina* demonstrates a capacity to withstand harsh growth conditions, including arid, saline, and alkaline environments, thereby mitigating the risk of contamination during fermentation [27]. Shinorine, a UV-absorbing mycosporine-like amino acid (MAA), has demonstrated potential for use in sunscreen applications [28]. MAAs are synthesized by a range of prokaryotic and eukaryotic organisms, including cyanobacteria, fungi, and algae [29]. Although shinorine is commercially available from the red algae *Porphyra umbilicalis*, its low productivity limits broader application use [30]. In addressing this challenge, a range of host organisms, including *Es. coli* [31], *Saccharomyces cerevisiae* [32], *Corynebacterium glutamicum* [33], and *P. putida* [34], have been genetically engineered to enhance shinorine production. However, the complex fermentation process, along with challenges in extraction and purification, hinders its practical application. Consequently, there is a necessity to explore alternative and sustainable methods for large-scale shinorine production [34].

In this study, a highly efficient and user-friendly CRISPR-Cas9 system was developed for *E. persicina*. This system facilitates expeditious and precise gene editing, enabling the knockout of a 42 kb genomic fragment and the insertion of genes controlled by strong promoters. The system can be efficiently cured through sucrose counter-selection and supports iterative genome editing. Furthermore, the entire 6.4 kb shinorine biosynthetic gene cluster was successfully integrated into *E. persicina* using CRISPR-Cas-mediated editing combined with conjugative transfer. These methods will facilitate future research on the pathogenic mechanisms of *E. persicina* and its metabolic engineering, including the production of andrimid, pink pigments, and shinorine [5,35]. The findings of this study offer valuable insights into the broader application of CRISPR-Cas systems in other microorganisms.

2. Materials and methods

2.1. Strains and culture conditions

The strains used in this study are enumerated in Tables S1 and Eand *E. persicina* BST187 has been deposited in the China Center for Type Culture Collection (CCTCC) with accession number CCTCC M 2022872. All strains were cultivated on Luria-Bertani (LB) agar medium (5 g/L yeast extract, 10 g/L tryptone, 5 g/L NaCl, and 15 g/L agar) and incubated at 28 °C or 37 °C with agitation at 200 rpm for propagation. When necessary, 50 μg/mL kanamycin, 100 μg/mL ampicillin, 100 μg/mL X-gal (Solarbio, China), and 20 mM L-arabinose were supplemented in the medium.

2.2. Plasmid construction

The plasmids used in this study are enumerated in Table S2, while the primers are detailed in Table S3. The *Es. coli* codon-optimized genes of Ava_3855, Ava_3856, Ava_3857, and Ava_3858, as described in *Anabaena variabilis* [31] were synthesized by GenScript Biotech Corporation (China). Primers were synthesized by GENEWIZ (China), and DNA fragments were amplified using KOD One™ PCR Master Mix (TOYOBO, Japan). Plasmids were constructed via Gibson assembly using the EZ-HiFi Seamless Cloning Kit (GenStar, China) [36]. Restriction endonuclease *Bsa*I-HF®v2 and T4 DNA ligase, used for Golden Gate assembly, were purchased from New England Biolabs (USA). The New Gel Mini Purification kit and Fast Plasmid Miniprep kit were purchased from ZOMANBIO (China).

The primers cas-J23119-lacZ-F and cas-J23119-lacZ-R were employed to replace the gRNA's native promoter with J23119. The multi-gRNA plasmid was constructed by Golden Gate assembly using Cas9-Δ*lacZ*-pJ23119-gRNA0 (gRNA5) as the backbone. The iterative plasmid Cas9-pSC101-*sacB*-Δ*adhE* was also constructed using gRNA5 as the backbone, with the *sacB* and *oriT* sequences being amplified from the plasmid pK18mobsacB. The conjugative transfer plasmid Cas9-*oriT*-*sacB*-*lacI*-*admT*-pJ23119-Δ*lacZ* (gRNA7) was constructed using Cas9-*oriT*-*sacB*-pJ23119-Δ*lacZ* (gRNA6) as the backbone. The *oriT*, *admT*, and *lacI* genes were amplified from pK18mobsacB, pJ23104-*admX*, and pET28a, respectively. Subsequently, the upstream and downstream homology arms of *lacI2* and the MAAs gene were integrated into gRNA7, thereby producing the final plasmid, Cas9-*oriT*-*admT*-Δ*lacI*::Ptrc-MAAs (gRNA8). Detailed information, including templates and fragment sizes for each plasmid, is provided in Table S2. Finally, all reaction products were chemically transformed into *Es. coli* DH5α, and Sanger sequencing (GENEWIZ, China) was employed to evaluate the accuracy of the assembly.

2.3. Transformation

The chemical competent cells of BST187 were prepared using 0.1 M $CaCl_2$ and 50 % glycerol, as previously described [16]. The preparation of BST187 electroreceptor competent cells involved the use of sterile ddH_2O and 10 % glycerol, and these cells were subsequently stored in 10 % glycerol. The chemical transformation was performed via heat

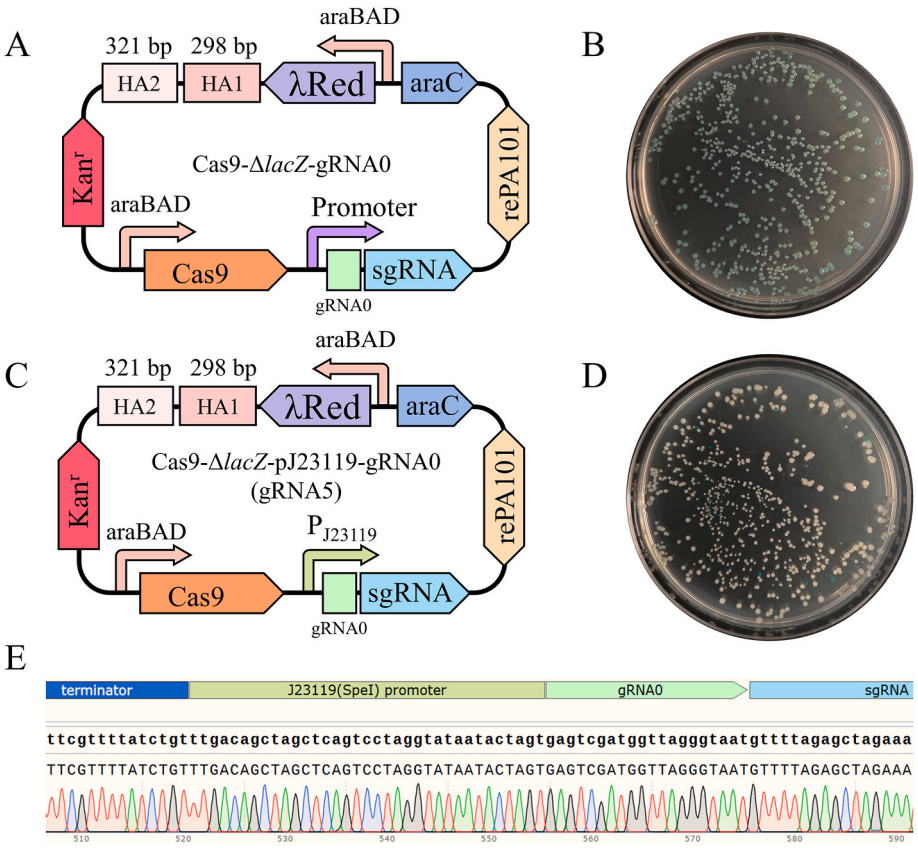

Fig. 1. Establishment of the high-level sgRNA expression using a CRISPR-Cas9-based toolkit in BST187. (A) Schematic representation of the Cas9-Δ*lacZ*-gRNA0 plasmid. (B) Colony images of BST187 containing the Cas9-Δ*lacZ*-gRNA0 plasmid, cultivated on LB plates supplemented with X-gal, kanamycin, ampicillin, and L-arabinose. White colonies signify successful knockout strains, while blue colonies denote unsuccessful outcomes. (C) Schematic representation of the Cas9-Δ*lacZ*-pJ23119-gRNA0 plasmid. (D) Colony images of BST187 containing the Cas9-Δ*lacZ*-pJ23119-gRNA0 plasmid, which were cultivated under the same conditions as in panel B. (E) Sanger sequencing confirming the replacement of the native sgRNA promoter with J23119.

shock, while electroporation was carried out using the Gene Pulser Xcell™ electroporation system (Bio-RAD, USA). A total of 100 mL of competent cells was mixed with approximately 500 ng of plasmid DNA in a 2-mm Gene Pulser cuvette. The optimized parameters for this process were as follows: a voltage setting of 2,000 V, resistance of 200 Ω, and capacitance of 25 μF. The cell suspension was then immediately placed into 1 mL of ice-cold LB medium, and the cells were incubated for 1 h at 28 °C with shaking at 200 rpm. Following this, the cells were plated on solid LB medium that had been supplemented with kanamycin, ampicillin, and 1 % glucose.

For large plasmids (≥15 kb), *Es. coli* S17-1 was employed as a donor strain, and standard conjugation methods, as described in a previous study [35], were utilized. Subsequent to the transformation of the plasmids into *E. persicina* BST187, the resultant BST187 strains containing CRISPR-Cas9 plasmids were cultivated on LB plates that had been supplemented with kanamycin, ampicillin and 1 % glucose.

2.4. Genome editing procedure

A correctly identified clone was selected and inoculated into LB medium, which had been supplemented with kanamycin and ampicillin. Following this, the medium was subjected to incubation for 4 h at 28 °C. Subsequently, 20 mM L-arabinose was added. Following a 12 h of induction, the culture was diluted 1,000-fold with 0.85 % NaCl, and 100 μL of the dilution was plated onto LB agar containing kanamycin, ampicillin, and L-arabinose. The plates were incubated for 24 h at 28 °C. Colonies obtained from the plates were subsequently inoculated into 500 μL of LB broth and incubated at 200 rpm for 10–12 h at 28 °C.

In instances where *lacZ* was used as the target gene, X-gal was incorporated into the LB agar plates at a final concentration of 100 μg/mL. Following a 24 h of incubation, white colonies were identified as successful knockout strains, while blue colonies were considered unsuccessful. The editing efficiency was calculated as the ratio of white colonies to the total number of colonies. The editing efficiency of other genes and insertion fragments was assessed using colony PCR with a forward primer upstream of the left homology arm and a reverse primer downstream of the right homology arm. Colonies that exhibited the expected PCR products then subjected to further verification DNA sequencing.

2.5. Plasmid curing

In order to cure the temperature-sensitive plasmid, the edited strains were grown overnight at 37 °C [37]. For the curing of the *sacB* counter-selectable marker plasmid, these strains underwent a 1,000-fold dilution in 0.85 % NaCl, followed by streaking onto LB agar plates containing 15 % sucrose. These plates were then incubated overnight at 28 °C. Colonies that grew on these plates were then inoculated into 500 μL of LB broth containing 15 % sucrose and incubated with shaking at 200 rpm overnight at 28 °C. The curing of the plasmid was confirmed by assessing the strain's sensitivity to kanamycin prior to proceeding with the next round of genome editing.

2.6. In vivo assay for andrimid sensitivity

The sensitivity to andrimid was assessed using modified agar lawn assays [38]. Briefly, 100 mL of LB agar plates were prepared by adding 1 mL of an overnight culture of *Es. coli* S17-1 strain, which had been

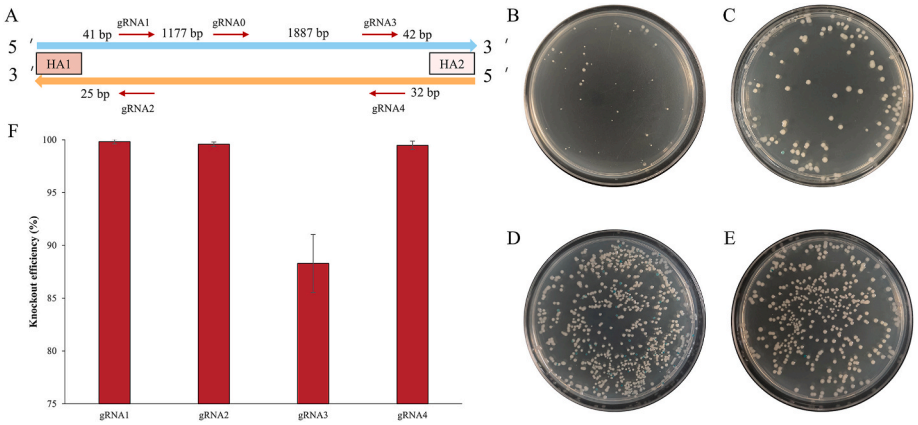

Fig. 2. Knockout efficiency of the CRISPR-Cas9 method in targeting the *lacZ* using different gRNA designs. (A) Schematic representation of five different gRNA designs, with their targeting positions. (B) Colony images of BST187 containing the Cas9-Δ*lacZ*-gRNA1 plasmid, cultivated on LB plates supplemented with X-gal, kanamycin, ampicillin, and L-arabinose. (C) Colony images of BST187 containing the Cas9-Δ*lacZ*-gRNA2 plasmid, cultivated under the same conditions as panel B. (D) Colony images of BST187 containing the Cas9-Δ*lacZ*-gRNA3 plasmid, cultivated under the same conditions as panel B. (E) Colony images of BST187 containing the Cas9-Δ*lacZ*-gRNA4 plasmid, cultivated under the same conditions as panel B. (F) Knockout efficiency based on the number of positive (white) colonies. White colonies signify successful knockout strains, while blue colonies denote unsuccessful outcomes. Values represent the means of biological replicates, with error bars indicating the standard deviations of three biological replicates.

transformed with CRISPR-Cas9 plasmids. A 2.5 μL aliquot of the BST187 culture was then spotted onto the LB agar plates. Following drying in a clean bench, the plates were then incubated at 28 °C for 2 days.

2.7. Identification and quantification of shinorine

The shinorine-producing strain was cultivated in 100 mL of LB medium in a 250 mL flask, which was then incubated for 24 h at 28 °C with shaking at 230 rpm. The samples were then homogenized using a High Pressure Homogenizer (AH-NANO, DUONING, China) in order to quantify the total shinorine. In addition, 1 mL of the untreated sample was used to quantify the extracellular shinorine. Subsequent to this, all samples were subjected to centrifugation at 13,000 rpm for 5 min, and the supernatant was filtered through a 0.22 μm filter. Qualitative analysis was then conducted using UPLC-TOF-MS/MS, with detected by a Shimadzu Nexera ultra-performance liquid chromatography (UPLC) 30A (Shimadzu, Japan) coupled with a TripleTOF™ 6600 mass spectrometer (Applied Biosystem Sciex, USA). The MS method incorporated a TOF MS scan and an IDA-fragmentation TOF MS/MS scan, covering a mass range of 50–1,000 *m/z* in positive electrospray ionization (ESI) mode. The samples were performed on a T3 column (Waters, 2.1 × 100 mm, 1.8 μm, 100 Å). The injection volume was set to 1 μL, and the column temperature was maintained at 30 °C. The mobile phases comprised 0.1 % formic acid in water (A) and acetonitrile (B). The flow rate was set to 0.3 mL/min with a gradient elution profile: 0.01 min, 1 % B; 1.5 min, 1 % B; 15–20 min, 99 % B; 21–30 min, 1 % B. The ESI source parameters were optimized as follows: ion spray voltage of 4,500 V, declustering potential of 80 V, source temperature of 550 °C, curtain gas at 35 psi, nebulizer gas at 55 psi, and heater gas at 55 psi. The raw data (.wiff) files were processed and analyzed using PeakView software for peak detect and alignment.

For the purpose of quantitative analysis, the shinorine-producing strain was also analysis by HPLC. Samples were injected onto a SHIMADZU LC-2050 system equipped with a Thermo HyperCarb column (100 × 4.6 mm, 5 μm). A sample injection volume of 20 μL was used, and the column temperature was maintained at 25 °C. The mobile phases consisted of 0.3 % ammonium formate in water at pH 9.0 (A) and acetonitrile (B). The flow rate was set to 1.5 mL/min with a gradient elution: 0 min, 2 % B; 20 min, 15 % B; 26 min, 50 % B; 27–33 min, 90 % B; 35–40 min, 2 % B. Detection was carried out at a wavelength of 334 nm [34].

3. Results and discussion

3.1. Optimization of CRISPR-Cas9 knockout in BST187

The protocol was established through adapting the one-plasmid system developed by Zhao et al. [37] for use in *E. persicina* BST187, in which Cas9 and sgRNA are co-expressed on a single plasmid. This system includes the Cas9 gene, which encodes the Cas9 protein responsible for inducing DSBs in the target DNA, and the sgRNA, which guides Cas9 to the target sequence. The non-essential *lacZ* gene was selected as the target for genome editing in *E. persicina* BST187, due to its utility as a color reporter on X-gal plates [16]. However, no positive strains were obtained following L-arabinose induction (Fig. 1AB). The failure to obtain positive strains may be due to inappropriate Cas9/sgRNA expression levels. Specifically, low levels of sgRNA expression have been shown to reduce the number of Cas9/sgRNA complexes, thereby hindering effective cleavage at the target site [39]. Conversely, studies have indicated that high levels of sgRNA expression can enhance target knockout efficiency in *Yarrowia lipolytica* [40], *Halomonas* spp. [41], and mammalian cells [39]. Li et al. [18] developed a CRISPR-Cas9-based cytosine base editing system in *E. amylovora*, in which the sgRNA was expressed under the control of the synthetic promoter J23119. The strength of the sgRNA promoter remains unclear in the pRed_Cas9_Δ*poxB*300 plasmid [37]. Consequently, J23119 was selected to drive sgRNA expression in *E. persicina* BST187 (Fig. 1C–E). The use of this strong promoter ensured the effective genome editing in *E. persicina* BST187, yielding an efficiency of 92.66 ± 2.13 %, even in instances where the distance from the PAM sequence to the nearest homology arm (PAM-to-HA) exceeded 1,000 bp.

Furthermore, studies have demonstrated that DSBs in close proximity to the donor DNA facilitate homology-directed repair (HDR) [42,43]. In order to design sgRNAs for CRISPR-Cas9, five sgRNAs (gRNA0, gRNA1, gRNA2, gRNA3, and gRNA4) targeting *lacZ* were tested. Of these, four sgRNAs (gRNA1, gRNA2, gRNA3 and gRNA4) were located within 50 bp of the proximal homology arm sequence, while gRNA0 was positioned more than 1,000 bp away (Fig. 2A) [20]. Following a 48 h incubation, the knockout efficiency of *lacZ* was assessed by enumerating the number of positive colonies on the plate (Fig. 2B–E). The knockout efficiencies were as follows: gRNA1 (99.82 ± 0.21 %), gRNA2 (99.57 ± 0.22 %), gRNA4 (99.47 ± 0.41 %), and gRNA3 (88.28 ± 2.76 %). In contrast to the 26 % editing efficiency achieved by suicide plasmids [16], the majority of sgRNAs exhibited near-100 % knockout efficiency,

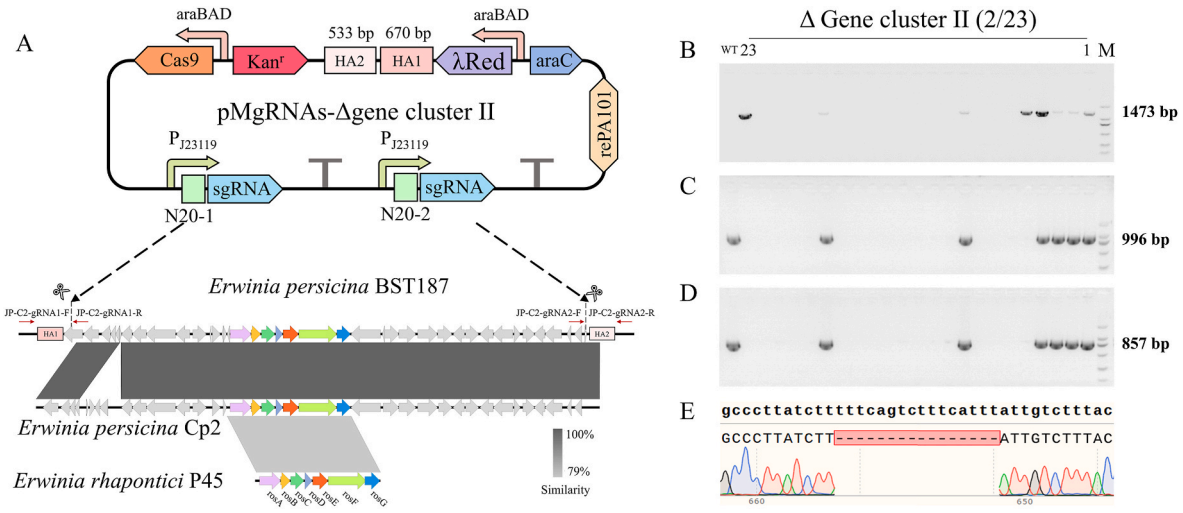

Fig. 3. Knockout efficiency of the CRISPR-Cas9 method targeting gene cluster II in BST187. (A) Schematic representation of the plasmid pMgRNAs-Δgene cluster II, with genome comparison visualized using Easyfig. (B) PCR analysis showing the deletion of gene cluster II in BST187 using primers JP-C2-gRNA1-F and JP-C2-gRNA2-R. (C) PCR analysis showing the deletion of gene cluster II in BST187 using primers JP-C2-gRNA1-F and JP-C2-gRNA1-R. (D) PCR analysis showing the deletion of gene cluster II in BST187 using primers JP-C2-gRNA2-F and JP-C2-gRNA2-R. (E) Sanger sequencing results confirming the knockout of gene cluster II in BST187.

with gRNA3 being the exception (Fig. 2F). In addition to *lacZ*, the *adhE* gene was selected for comparison of the editing efficiency of suicide plasmids and CRISPR-Cas9 methods for the same cargo. As demonstrated in Fig. S1, the editing efficiency was only 30.4 % (7/23, Fig. S1AB) using suicide plasmids in BST187. Conversely, the utilization of CRISPR-Cas9 plasmids resulted in the successful generation of *adhE* knockout strains, with an editing efficiency of 95.7 % (22/23, Fig. S1CD) in BST187. This study emphasizes the importance of sgRNA design, and the current CRISPR-Cas9 system demonstrates enhanced editing efficiency in *E. persicina*, making it suitable for subsequent genome editing.

3.2. Large fragment deletion

In order to evaluate the efficacy of the CRISPR–Cas9 system in knocking out longer DNA segments from BST187, we expressed multiple sgRNAs on a single plasmid [44,45]. Gene cluster II is involved in the biosynthesis of the Fe^{2+} chelator proferrorosamine A, which theoretically competes with andrimid biosynthesis (Fig. S2) [46] and is considered as a potential virulence factor [47]. Consequently, gene cluster II was selected to assess the efficiency of large fragment knockout. The double sgRNA plasmid was constructed using *Bsa*I-mediated enzymatic digestion and schematic representations of the plasmid construction and knockout sites are depicted in Fig. 3A. Both sgRNAs are expressed under the control of the constitutive promoter J23119.

Following L-arabinose induction, the knockout efficiency was assessed using the primers JP-C2-gRNA1-F and JP-C2-gRNA2-R. The positive strains exhibited a band at 1,473 bp, while no band was observed in the negative strains (Fig. 3B). Among the 23 colonies examined, eight displayed the expected band, while four showed clear bands. Subsequent validation using the JP-C2-gRNA1-F/JP-C2-gRNA1-R and gRNA2-F/JP-C2-gRNA2-R primers revealed that some of the positive strains also exhibited wild-type bands (Fig. 3CD). Ultimately, two successful knockout strains, CII-5 and CII-23, were identified. The confirmation of these strains was further substantiated by Sanger sequencing (Fig. 3E), which confirmed the successful knockout of a 42,892 bp DNA fragment, thereby achieving a knockout efficiency of

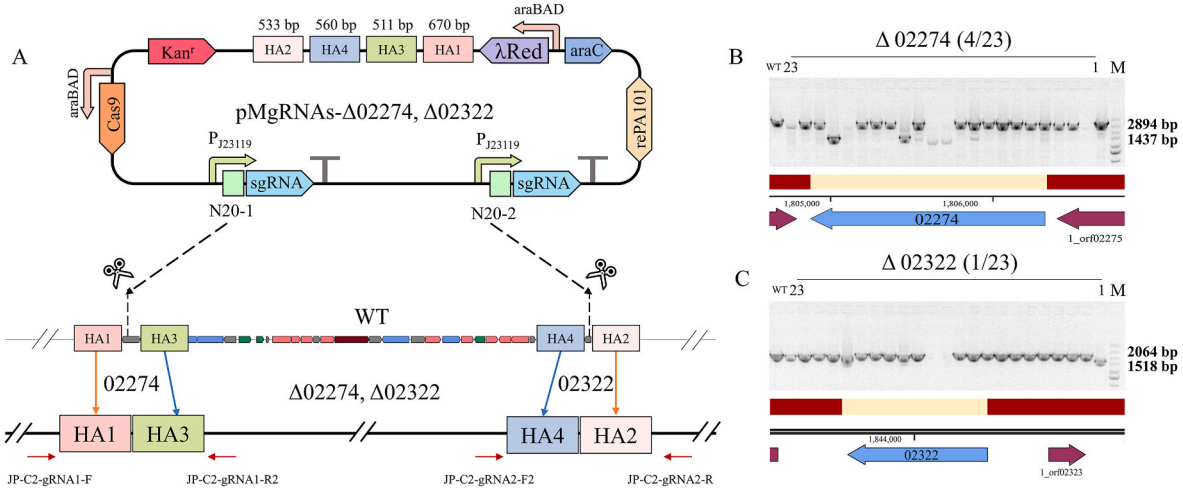

Fig. 4. Knockout efficiency of the CRISPR-Cas9 method in BST187, targeting genes 02274 and 02322 within gene cluster II. (A) Schematic representation of the plasmid pMgRNAs-Δ02274, Δ02322, targeting genes 02274 and 02322. (B) PCR analysis and Sanger sequencing confirming the targeted deletion of gene 02274 in BST187 using primers JP-C2-gRNA1-F and JP-C2-gRNA1-R2. (C) PCR analysis and Sanger sequencing confirming the targeted deletion of gene 02322 in BST187 using primers JP-C2-gRNA2-F2 and JP-C2-gRNA2-R.

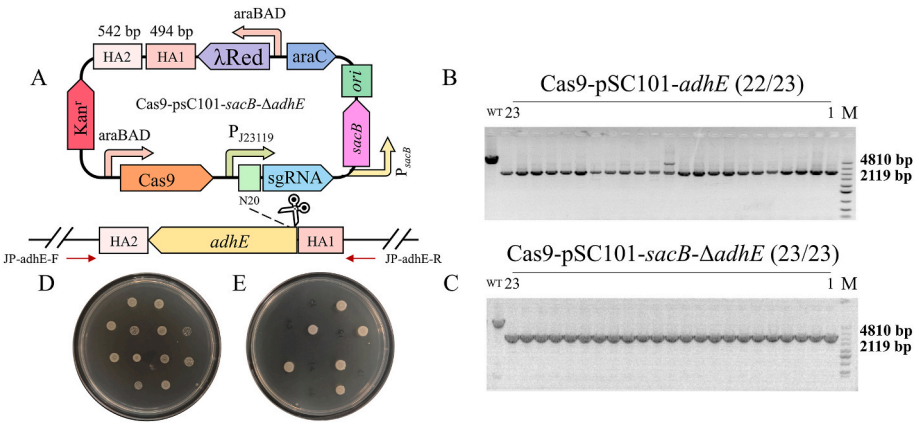

Fig. 5. Development of an iteratively editable plasmid in BST187 targeting the *adhE* gene (the size of the *adhE* band is 2,691 bp, with the expected fragment size for the wild-type band generated by PCR being 4,810 bp, and the size of the successful knockout strain being 2,119 bp). (A) Schematic representation of the plasmid Cas9-pSC101-*sacB*-Δ*adhE*. (B) PCR analysis of the *adhE* targeted deletion in BST187 using primers JP-adhE-F and JP-adhE-R based on the plasmid Cas9-pSC101ts-Δ*adhE* (C) PCR analysis of the *adhE* targeted deletion in BST187 using primers JP-adhE-F and JP-adhE-R based on the plasmid Cas9-pSC101-*sacB*-Δ*adhE*. (D) Validation of residual resistance in Cas9-pSC101ts-Δ*adhE* knockout plasmid strains. (E) Validation of residual resistance in Cas9-pSC101-*sacB*-Δ*adhE* knockout plasmid strains, with no colony growth on LB plates containing kanamycin indicating plasmid loss.

8.7 %. This efficiency is adequate for subsequent genome modifications, and the approach may be applied to knock out competing gene clusters and facilitate genome reduction [48].

3.3. Multiplex genome editing

The aforementioned method described above targets a single genomic locus at a time; however, simultaneous editing of multiple loci is often a prerequisite for the development of microbial cell factories. To achieve this, multiplexed sgRNAs can be utilized to target and modify multiple genomic loci in a simultaneous manner. Building on the large-fragment deletion plasmid pMgRNAs-Δgene cluster II, we constructed the double-gene knockout plasmid pMgRNAs-Δ02274, Δ02322 was constructed, targeting genes 02274 and 02322 (Fig. 4A).

Following L-arabinose induction, the primers JP-C2-gRNA1-F/JP-C2-gRNA1-R2 and JP-C2-gRNA2-F2/JP-C2-gRNA2-R were employed to assess the knockout efficiency. For gene 02274, the target fragment was 1,443 bp, the wild-type fragment was 2,894 bp, and the successful knockout product was 1,457 bp (Fig. 4B). For gene 02322, the target fragment was 546 bp, while the wild-type fragment was 2,064 bp, and the successful knockout product was 1,518 bp (Fig. 4C). Unfortunately, simultaneous knockout of both genes was not achieved, which insufficient Cas9 protein expression under the L-arabinose-inducible pBAD promoter [49]. Furthermore, colonies II-2, II-12, II-13 and II-19 exhibited neither successful editing nor wild-type bands, which may be attributable to the activation of alternative end-joining (A-EJ), a repair pathway analogous to non-homologous end joining [50].

3.4. Plasmid curing

In order to implement a one-plasmid system for multiple rounds of genome editing, it is necessary to cure plasmids that carry resistance, with the *adhE* gene being selected for knockout. Following the generation of the Δ*adhE* strain, the editing plasmid Cas9-pSC101ts-Δ*adhE* was

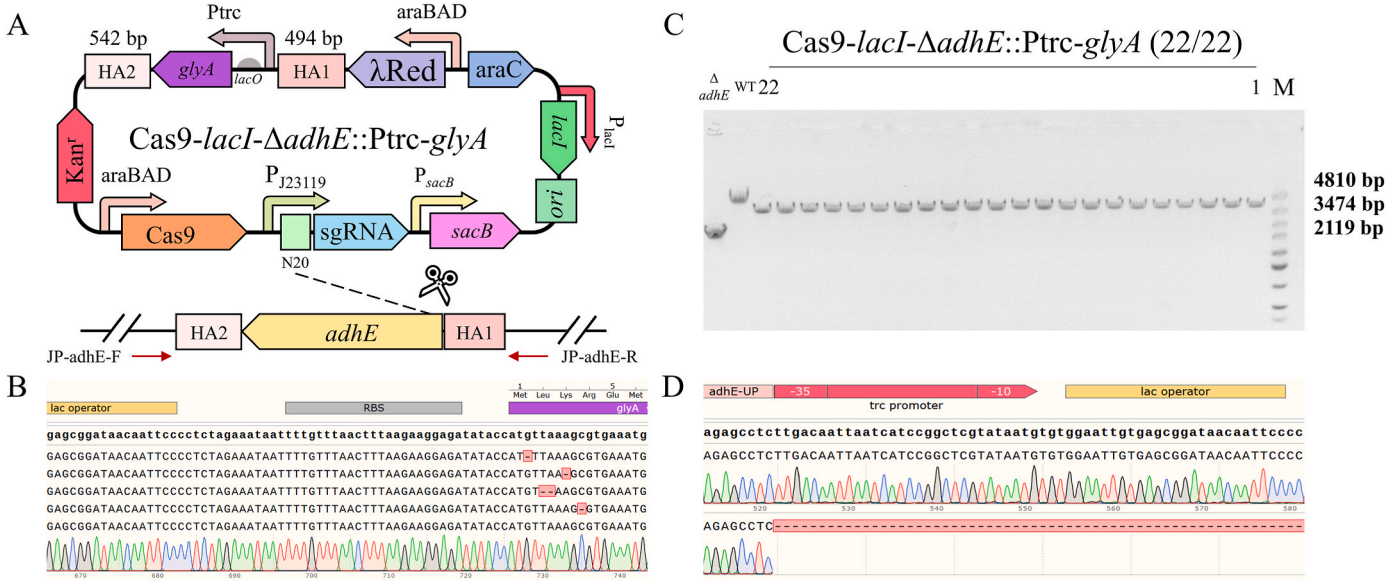

Fig. 6. Insertion of highly expressed genes into BST187. (A) Schematic representation of the plasmid Cas9-*lacI*-Δ*adhE*::Ptrc-*glyA*. (B) Sanger sequencing results show that insertion of the *lacI* gene produced an unmutated Cas9-*lacI*-Δ*adhE*::Ptrc-*glyA* plasmid. (C) PCR analysis confirming the insertion of Ptrc-*glyA* at the *adhE* locus in BST187 using primers JP-adhE-F and JP-adhE-R. (D) Sanger sequencing results confirming the successful insertion of the Ptrc-*glyA* gene at the *adhE* locus.

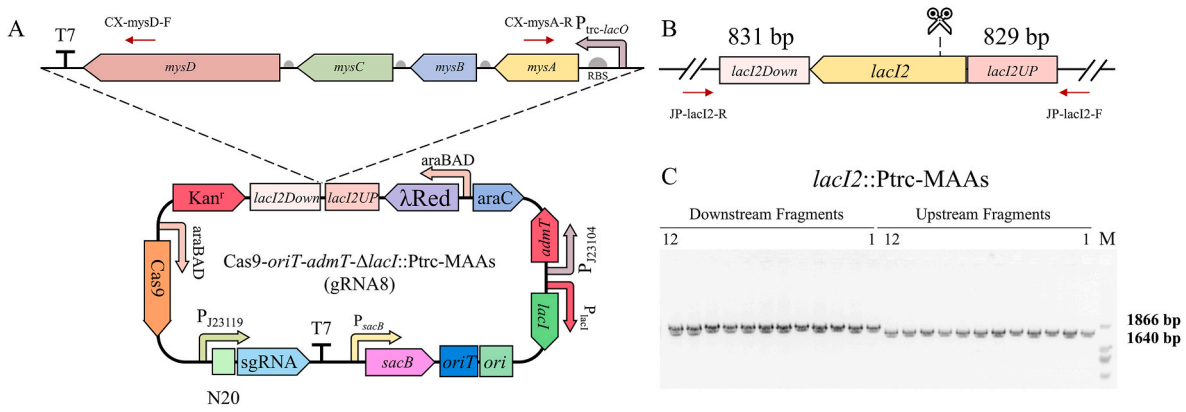

Fig. 7. Insertion of a large DNA fragment into BST187. (A) Schematic representation of the Cas9-*oriT*-*admT*-Δ*lacI*::Ptrc-MAAs (gRNA8). (B) Schematic representation of insertion site at *lacI2*. (C) PCR analysis confirming the targeted insertion of Ptrc-MAAs into BST187 using primers JP-lacI2-F/CX-mysA-R and CX-mysD-F/JP-lacI2-R.

cured by culturing the colonies for 24 h at 37 °C. The efficacy of this process was then assessed by plating the colonies on LB plates containing kanamycin and incubating for a further 24 h at 28 °C. However, BST187 exhibited reduced growth at 37 °C. In order to enhance plasmid curing efficiency, the sucrose-sensitive *sacB* gene was incorporated into the plasmid as a selection marker that is widely used [20,51]. Additionally, the temperature-sensitive replicon pSC101ts was replaced with the pBR322 replicon from pK18mobsacB, which proved to be more time-efficient (Fig. 5A) [21]. Following L-arabinose induction, plasmid curing of Cas9-psC101-*sacB*-Δ*adhE* was carried out by incubating the culture overnight at 28 °C in LB medium supplemented with 15 % sucrose [16]. A 2.5 μL aliquot of the culture, which contained a PCR product with a band size of 2,119 bp (Fig. 5BC), was plated onto LB agar containing kanamycin and incubated at 28 °C for 24 h.

All temperature-sensitive plasmids exhibited residual resistance (Fig. 5D), while the curing rate using *sacB* as a counter-selection marker was 56.52 % (13/23, Fig. 5E). The iterative plasmid allows *Es. coli* strains to grow at their optimal temperature, thereby shortening the timeline of the genome editing protocol. Furthermore, this method eliminates the need for *Es. coli* S17-1 in conjugative transfer, saving at least three days per round of gene editing compared to the use of suicide plasmids [16].

3.5. Highly expressed genes insertion

In order to evaluate the genome editing method's capacity for mediate fragment insertion, an attempt was made to insert *glyA* fragments into the *adhE* locus of BST187. As demonstrated in Fig. 6A and B, mutations in the promoter and upstream region of the *glyA* gene suggest that the expression of this gene under Ptrc regulation is toxic. The repressive effect of lacO on Ptrc was enhanced by incorporating the *lacI* element into the plasmid. The lacI-encoded has been demonstrated to bind to lacO with high efficiency, thereby preventing leaky expression. This has enabled the successful acquisition of the unmutated plasmid.

The promoter region and the *gly* gene together span 1,355 bp. After L-arabinose induction, the expected PCR product size was 3,474 bp. PCR analysis revealed that 22 strains exhibited the expected fragment size (Fig. 6C). Sanger sequencing of the PCR products further confirmed the successful integration of Ptrc-*gly* (Fig. 6D). The integration of a single exogenous gene into the target locus was achieved with 100 % efficiency, fulfilling the requirements for subsequent experiments.

3.6. Large fragment insertion

The transformation efficiency of the CRISPR-Cas9 plasmid was significantly improved through electroporation in BST187 (32.67 ± 4.16 CFU/μg) in comparison with chemical transformation (4.67 ± 1.16 CFU/μg). However, no successful transformants were obtained when the plasmid size exceeded approximately 15 kb. Conjugative transfer is widely considered the preferred method for introducing large exogenous DNA into non-model bacteria [23,52]. Conjugative transfer plasmids generally contain at least an origin of transfer (*oriT*) sequence and a gene encoding relaxase. The conjugative plasmid gRNA6 was constructed using gRNA5 as the backbone, incorporating the transfer initiation site *oriT* and the counter-selection marker *sacB*. Furthermore, the incorporation of a self-resistance gene fragment into the plasmid and the enhanced expression of *admT* significantly improved *Es. coli* S7-1 resistance to andrimid, consistent with previous studies [38]. Ultimately, the Cas9-*oriT*-*sacB*-*lacI*-*admT*-pJ23119-Δ*lacZ* (gRNA7) plasmid was successfully constructed (Fig. S3A). A point mutation in the *admT* gene altered its start codon from AUG to AUA (Fig. S3B). The inhibitory effect of BST187 in S17-1 containing the gRNA7 plasmid was significantly reduced compared to that in S17-1 containing the gRNA6 plasmid (Fig. S3C). Indeed, AUA as a start codon produced only 1–3 % of the protein yields relative to AUG [53]. In order to mitigate the effect of such mutations, the strength of the *admT* promoter could be reduced. Furthermore, *admT* has been identified as a promising candidate as a new resistance marker. Finally, the gRNA7 plasmid has been successfully introduced into BST187 by conjugative transfer.

Subsequently, the upstream and downstream homology arms, in conjunction with the N20 region, were substituted using gRNA7 as the backbone. Moreover, the *lacI2* gene was substituted with a Ptrc-MAAs fragment (6408 bp), thereby facilitating gene expression under the control of the Ptrc promoter. The final size of the Cas9-*oriT*-*admT*-Δ*lacI*::Ptrc-MAAs (gRNA8) plasmid was 22,829 bp (Fig. 7AB). The gRNA8 plasmid was successfully transformed into two distinct genetic backgrounds of BST187 (wild-type and Δ*admX*) using the donor strain S17-1. Following L-arabinose induction, twelve strains from each genetic background were randomly selected for PCR analysis, which revealed the expected PCR fragment sizes of 1,640 bp and 1,866 bp, respectively. The insertion efficiency of the large fragments into the different genetic backgrounds was 100 % (Fig. 7C). The plasmid curing efficiencies for the wild-type and the Δ*admX* strains were 36.4 % and 33.3 %, respectively.

3.7. Shinorine production in E. persicina

The analysis of the supernatant samples was conducted using UPLC-TOF-MS/MS, and a peak with a retention time of approximately 1 min was detected in the BST187 strain, showing an *m/z* value of 333.1286 (Fig. S4A). The fragmentation pattern of this ion matched a previous report, with identified peaks at *m/z* 186.1 and 255.147 (Fig. S4B) [54]. The positive strains were further validated using HPLC analysis. The

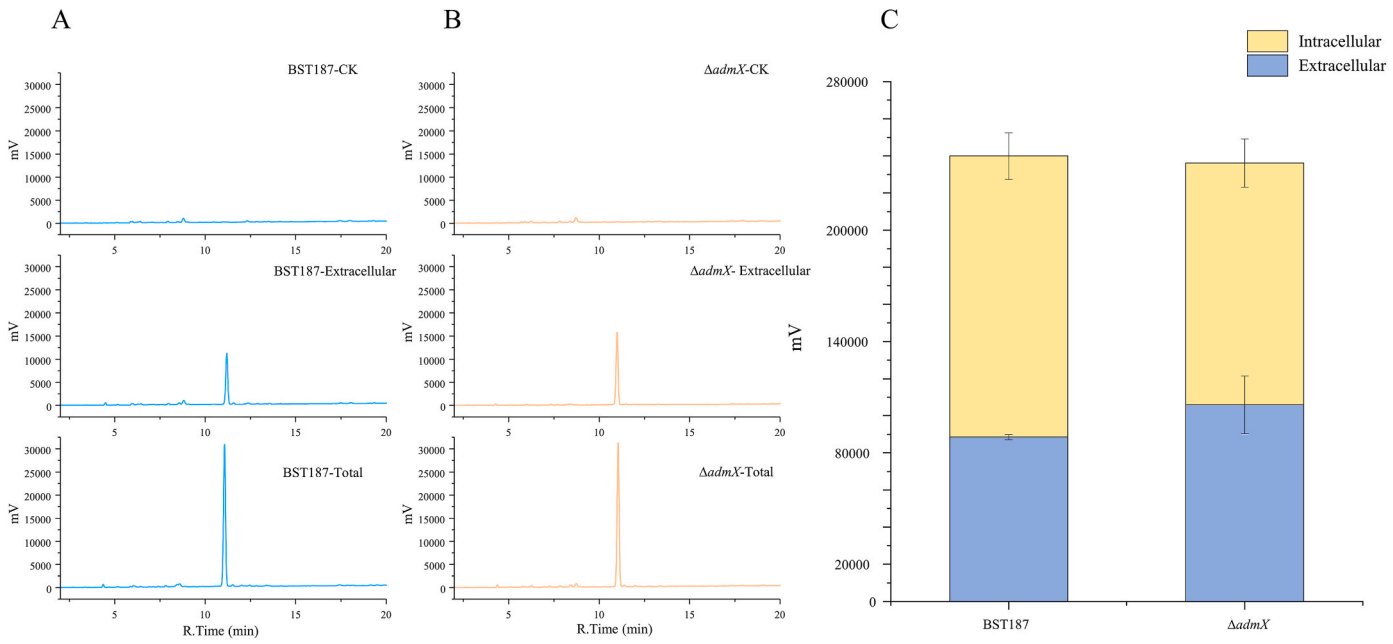

Fig. 8. Determination of shinorine production in *E. persicina*. (A) HPLC spectra of extracellular and total shinorine from the BST187 strain. (B) HPLC spectra of extracellular and total shinorine from the Δ*admX* strain. (C) Peak area of the 11-min unknown peak in the extracellular and intracellular fractions from the BST187 and Δ*admX* strains. Values represent the means of biological replicates, with error bars indicating the standard deviations of three biological replicates.

results showed that both the extracellular and total samples exhibited a new peak at approximately 11 min (Fig. 8AB). In the wild-type strain (BST187), the extracellular peak area was 88,512 mV, corresponding to approximately 36.9 % of the total area, while in the Δ*admX* strain, the extracellular peak area was 105,961 mV, representing approximately 44.9 % of the total area. No significant difference was observed between the two fractions from BST187 and Δ*admX* (Fig. 8C).

In contrast to *Fischerella* [54], BST187 does not require a phosphopantetheinyl transferase (PPTase) element for the production of shinorine, and it has a shorter fermentation time compared to *S. cerevisiae* [32], highlighting its potential for significant applications as a host for heterologous expression of secondary metabolites. This case demonstrates the potential application of our method in genome integration and metabolic engineering in *E. persicina*.

4. Conclusion

E. persicina has demonstrated promising characteristics, including the production of secondary metabolites, such as andrimid, pink pigment, and exopolysaccharides. However, effective, precise, and scarless gene-editing methods remain limited. In this study, we developed a rapid and efficient genome-editing method based on the CRISPR-Cas9 system in *E. persicina* BST187. Through the optimizing of sgRNA design and enhancement of sgRNA expression levels, we have achieved a high degree of precision in gene editing. Furthermore, large 42 kb genomic fragments of *E. persicina* have been successfully deleted using multiplexed sgRNAs. Concurrently, a 22 kb plasmid has been conjugally transferred into *E. persicina*, thus facilitating the insertion of large DNA fragments (6.4 kb) into BST187 for the production of shinorine. This work provides a framework for establishing effective gene-editing tools for microbial strains and demonstrates their potential as promising chassis for natural products production.

CRediT authorship contribution statement

Tingfeng Cheng: Writing – original draft, Visualization, Validation, Methodology, Investigation, Formal analysis, Data curation, Conceptualization. **Xinyan Cao:** Visualization, Validation, Methodology. **Yuchen Wang:** Visualization, Validation, Methodology. **Lei Zhao:** Writing – review & editing, Supervision, Resources, Investigation, Funding acquisition, Conceptualization.

Declaration of competing interest

The authors declare that they have no known competing financial interests or personal relationships that could have appeared to influence the work reported in this paper.

Acknowledgements

This project has received funding from the Hundred Talents Program of the Chinese Academy of Sciences to LZ (E3J56201).

Appendix A. Supplementary data

Supplementary data to this article can be found online at https://doi.org/10.1016/j.synbio.2025.02.006.

References

[1] Aremu B, Babalola O. Classification and taxonomy of vegetable Macergens. Front Microbiol 2015;6:1361. https://doi.org/10.3389/fmicb.2015.01361.
[2] Li WH, Jin DC, Li FL, Jin JX, Cheng Y. Phenotypic fingerprints of bacterium *Erwinia persicina* from larval gut of the diamondback moth, *Plutella xylostella* (Lepidoptera: Plutellidae). Acta Entomol Sin 2016;59:456. https://doi.org/10.16380/j.kcxb.2016.04.011.
[3] Bechtaoui N, Raklami A, Tahiri A, Benidire L, Göttfert M, Oufdou K. Phosphate-solubilizing rhizobacteria and their effects on the growth and phosphorus uptake by wheat plants. J Plant Nutr 2024;47:2811–23. https://doi.org/10.1080/01904167.2024.2369069.
[4] Deroo W, De Troyer L, Dumoulin F, De Saeger S, De Boevre M, Vandenabeele S, et al. A novel in Planta enrichment method employing Fusarium graminearum-infected wheat spikes to select for competitive biocontrol bacteria. Toxinst 2022; 14:222. https://doi.org/10.3390/toxins14030222.
[5] Zhang Y, Liu X, Li X, Zhao L, Zhang H, Jia Q, et al. Physicochemical properties and Antibiosis activity of the pink pigment of *Erwinia persicina* Cp2. Agric-BASEL 2022; 12:1641. https://doi.org/10.3390/agriculture12101641.
[6] Chen H, Jin Z, Huang R, He L, Tian W, Zhao L, et al. Promotion of growth of alfalfa by *Erwinia persicina* Cp2 exopolysaccharides under NaCl stress. Agron-BASEL 2023; 13. https://doi.org/10.3390/agronomy13082129.

[7] Cheng T, Ge T, Zhao L, Hou Y, Xia J, Zhao L. Improved production of andrimid in *Erwinia persicina* BST187 strain by fermentation optimization. BMC Microbiol 2023;23. https://doi.org/10.1186/s12866-023-02946-2.

[8] Kim W, Choi S, Han I, Cho S, Lee Y, Kim S, et al. Inhibition of *Salmonella enterica* growth by competitive exclusion during early alfalfa sprout development using a seed-dwelling *Erwinia persicina* strain EUS78. Int J Food Microbiol 2020;312:108374. https://doi.org/10.1016/j.ijfoodmicro.2019.108374.

[9] Mansfield J, Genin S, Magori S, Citovsky V, Sriariyanum M, Ronald P, et al. Top 10 plant pathogenic bacteria in molecular plant pathology. Mol Plant Pathol 2012;13:614–29. https://doi.org/10.1111/j.1364-3703.2012.00804.x.

[10] Orel D, Oguz E. Parsley (*Petroselinum crispum*) leaf and stem spot caused by *Erwinia persicina*. J Plant Pathol 2023;105:1539–49. https://doi.org/10.1007/s42161-023-01484-0.

[11] Galvez L, Gil-Serna J, Garcia-Diaz M, Palmero D. First report of a garlic bulb rot caused by *Erwinia persicina* in Europe. Plant Dis 2015;99:723–4. https://doi.org/10.1094/PDIS-11-14-1195-PDN.

[12] Cho H, Park JY, Kim YK, Sohn S-H, Park DS, Kwon Y-S, et al. Whole-genome sequence of *Erwinia persicina* B64, which causes pink soft rot in onions. Microbiol Resour Announc 2019;8:e01302. https://doi.org/10.1128/MRA.01302-18.

[13] Wang J, Han W, Pan Y, Zhang D, Zhao D, Li Q, et al. First report of *Erwinia persicina* causing stalk rot of celery in China. Plant Dis 2022;106:1514. https://doi.org/10.1094/PDIS-08-21-1723-PDN. 1514.

[14] Wasendorf C, Schmitz-Esser S, Eischeid C, Leyhe M, Nelson E, Rahic-Seggerman F, et al. Genome analysis of *Erwinia persicina* reveals implications for soft rot pathogenicity in plants. Front Microbiol 2022;13:1001139. https://doi.org/10.3389/fmicb.2022.1001139.

[15] Kawaguchi A, Abe D, Saito T, Nogata Y, Nomiyama K, Kohyama N, et al. Pink seed of barley caused by *Erwinia persicina*. J Gen Plant Pathol 2021;87:106–9. https://doi.org/10.1007/s10327-020-00974-8.

[16] Cheng T, Ge T, Zhao X, Liu Z, Zhao L. Efficient genetic transformation and suicide plasmid-mediated genome editing system for non-model microorganism *Erwinia persicina*. Bio-Protoc 2024;14:e4956. https://doi.org/10.21769/BioProtoc.4956.

[17] Ayora S, Carrasco B, Cárdenas PP, César CE, Cañas C, Yadav T, et al. Double-strand break repair in bacteria: a view from *Bacillus subtilis*. FEMS Microbiol Rev 2011;35:1055–81. https://doi.org/10.1111/j.1574-6976.2011.00272.x.

[18] Li C, Wang L, Cseke L, Vasconcelos F, Huguet-Tapia J, Gassmann W, et al. Efficient CRISPR-Cas9 based cytosine base editors for phytopathogenic bacteria. Commun Biol 2023;6. https://doi.org/10.1038/s42003-023-04451-8.

[19] Medina-Aparicio L, Dávila S, Rebollar-Flores J, Calva E, Hernández-Lucas I. The CRISPR-Cas system in Enterobacteriaceae. Pathog Dis 2018;76. https://doi.org/10.1093/femspd/fty002.

[20] Shukal S, Lim XH, Zhang C, Chen X. Metabolic engineering of *Escherichia coli* BL21 strain using simplified CRISPR-Cas9 and asymmetric homology arms recombineering. Microb Cell Fact 2022;21:19. https://doi.org/10.1186/s12934-022-01746-z.

[21] Li Q, Sun B, Chen J, Zhang Y, Jiang Y, Yang S. A modified pCas/pTargetF system for CRISPR-Cas9-assisted genome editing in *Escherichia coli*. Acta Biochim Biophys Sin 2021;53:620–7. https://doi.org/10.1093/abbs/gmab036.

[22] Volke DC, Orsi E, Nikel PI. Emergent CRISPR–Cas-based technologies for engineering non-model bacteria. Curr Opin Microbiol 2023;75:102353. https://doi.org/10.1016/j.mib.2023.102353.

[23] Vajente M, Clerici R, Ballerstedt H, Blank LM, Schmidt S. Using *Cupriavidus necator* H16 to provide a roadmap for increasing electroporation efficiency in Nonmodel bacteria. ACS Synth Biol 2024. https://doi.org/10.1021/acssynbio.4c00380.

[24] Bai S, Luo H, Tong H, Wu Y, Yuan Y. Advances on transfer and maintenance of large DNA in bacteria, fungi, and mammalian cells. Biotechnol Adv 2024;76:108421. https://doi.org/10.1016/j.biotechadv.2024.108421.

[25] Maese L, Rizzari C, Coleman R, Power A, van der Sluis I, Rau RE. Can recombinant technology address asparaginase *Erwinia chrysanthemi* shortages? Pediatr Blood Cancer 2021;68:e29169. https://doi.org/10.1002/pbc.29169.

[26] Tong W, Rizzari C. Back to the future: the amazing journey of the therapeutic anti-leukemia enzyme asparaginase *Erwinia chrysanthemi*. Haematologica 2023;108:2606–15. https://doi.org/10.3324/haematol.2022.282324.

[27] Zhang Z, Nan Z. *Erwinia persicina*, a possible new necrosis and wilt threat to forage or grain legumes production. Eur J Plant Pathol 2014;139:349–58. https://doi.org/10.1007/s10658-014-0390-0.

[28] Carreto JI, Carignan MO. Mycosporine-like amino acids: relevant secondary metabolites. Chemical and ecological aspects. Mar Drugs 2011;9:387.

[29] Geraldes V, Pinto E. Mycosporine-like amino acids (MAAs): biology, chemistry and identification features. Pharmaceuticals 2021;14. https://doi.org/10.3390/ph14010063.

[30] Hartmann A, Murauer A, Ganzera M. Quantitative analysis of mycosporine-like amino acids in marine algae by capillary electrophoresis with diode-array detection. J Pharm Biomed Anal 2017;138:153–7. https://doi.org/10.1016/j.jpba.2017.01.053.

[31] Balskus EP, Walsh CT. The genetic and molecular basis for sunscreen biosynthesis in cyanobacteria. Science 2010;329:1653–6. https://doi.org/10.1126/science.1193637.

[32] Kim S, Park B, Jin H, Lee D, Teoh J, Kim Y, et al. Efficient production of natural sunscreens shinorine, porphyra-334, and mycosporine-2-glycine in *Saccharomyces cerevisiae*. Metab Eng 2023;78:137–47. https://doi.org/10.1016/j.ymben.2023.05.009.

[33] Tsuge Y, Kawaguchi H, Yamamoto S, Nishigami Y, Sota M, Ogino C, et al. Metabolic engineering of *Corynebacterium glutamicum* for production of sunscreen shinorine. Biosci Biotechnol Biochem 2018;82:1252–9. https://doi.org/10.1080/09168451.2018.1452602.

[34] Yunus IS, Hudson GA, Chen Y, Gin JW, Kim J, Baidoo EEK, et al. Systematic engineering for production of anti-aging sunscreen compound in *Pseudomonas putida*. Metab Eng 2024;84:69–82. https://doi.org/10.1016/j.ymben.2024.06.001.

[35] Zhao L, Ge T, Cheng T, Wang Q, Cui M, Yuan H, et al. Fine-tuning gene expression of regulator AdmX for improved biosynthesis of andrimid in *Erwinia persicina* BST187. Appl Microbiol Biotechnol 2023;107:6775–88. https://doi.org/10.1007/s00253-023-12770-3.

[36] Gibson DG, Young L, Chuang R-Y, Venter JC, Hutchison CA, Smith HO. Enzymatic assembly of DNA molecules up to several hundred kilobases. Nat Methods 2009;6:343–5. https://doi.org/10.1038/nmeth.1318.

[37] Zhao D, Yuan S, Xiong B, Sun H, Ye L, Li J, et al. Development of a fast and easy method for *Escherichia coli* genome editing with CRISPR/Cas9. Microb Cell Fact 2016;15. https://doi.org/10.1186/s12934-016-0605-5.

[38] Liu X, Fortin P, Walsh C. Andrimid producers encode an acetyl-CoA carboxyltransferase subunit resistant to the action of the antibiotic. Proc Natl Acad Sci U S A 2008;105:13321–6. https://doi.org/10.1073/pnas.0806873105.

[39] Yuen G, Khan FJ, Gao S, Stommel JM, Batchelor E, Wu X, et al. CRISPR/Cas9-mediated gene knockout is insensitive to target copy number but is dependent on guide RNA potency and Cas9/sgRNA threshold expression level. Nucleic Acids Res 2017;45:12039–53. https://doi.org/10.1093/nar/gkx843.

[40] Schwartz CM, Hussain MS, Blenner M, Wheeldon I. Synthetic RNA polymerase III promoters facilitate high-efficiency CRISPR–Cas9-mediated genome editing in *Yarrowia lipolytica*. ACS Synth Biol 2016;5:356–9. https://doi.org/10.1021/acssynbio.5b00162.

[41] Qin Q, Ling C, Zhao Y, Yang T, Yin J, Guo Y, et al. CRISPR/Cas9 editing genome of extremophile *Halomonas* spp. Metab Eng 2018;47:219–29. https://doi.org/10.1016/j.ymben.2018.03.018.

[42] Liang X, Potter J, Kumar S, Ravinder N, Chesnut JD. Enhanced CRISPR/Cas9-mediated precise genome editing by improved design and delivery of gRNA, Cas9 nuclease, and donor DNA. J Biotechnol 2017;241:136–46. https://doi.org/10.1016/j.jbiotec.2016.11.011.

[43] Inui M, Miyado M, Igarashi M, Tamano M, Kubo A, Yamashita S, et al. Rapid generation of mouse models with defined point mutations by the CRISPR/Cas9 system. Sci Rep 2014;4:5396. https://doi.org/10.1038/srep05396.

[44] Feng X, Zhao D, Zhang X, Ding X, Bi C. CRISPR/Cas9 assisted multiplex genome editing technique in *Escherichia coli*. Biotechnol J 2018;13. https://doi.org/10.1002/biot.201700604.

[45] McCarty N, Graham A, Studená L, Ledesma-Amaro R. Multiplexed CRISPR technologies for gene editing and transcriptional regulation. Nat Commun 2020;11. https://doi.org/10.1038/s41467-020-15053-x.

[46] Born Y, Remus-Emsermann M, Bieri M, Kamber T, Piel J, Pelludat C. Fe^{2+} chelator proferrorosamine A: a gene cluster of *Erwinia rhapontici* P45 involved in its synthesis and its impact on growth of *Erwinia amylovora* CFBP1430. Microbiol-SGM 2016;162:236–45. https://doi.org/10.1099/mic.0.000231.

[47] Huang R, Zhang H, Chen H, He L, Liu X, Zhang Z. The determination of the biological function of bacterial pink pigment and *Fusarium chlamydosporum* on alfalfa (Medicago sativa L.). Front Microbiol 2023;14. https://doi.org/10.3389/fmicb.2023.1285961.

[48] Liu J, Zhou H, Yang Z, Wang X, Chen H, Zhong L, et al. Rational construction of genome-reduced Burkholderiales chassis facilitates efficient heterologous production of natural products from proteobacteria. Nat Commun 2021;12. https://doi.org/10.1038/s41467-021-24645-0.

[49] Ouellet B, Abdel-Mawgoud AM. Strong expression of Cas9 under a new 3′-truncated TEF1α promoter enhances genome editing in *Yarrowia lipolytica*. Curr Res Biotechnol 2023;6:100147. https://doi.org/10.1016/j.crbiot.2023.100147.

[50] Chayot R, Montagne B, Mazel D, Ricchetti M. An end-joining repair mechanism in *Escherichia coli*. Proc Natl Acad Sci U S A 2010;107:2141–6. https://doi.org/10.1073/pnas.0906355107.

[51] Huang C, Guo L, Wang J, Wang N, Huo Y. Efficient long fragment editing technique enables large-scale and scarless bacterial genome engineering. Appl Microbiol Biotechnol 2020;104:7943–56. https://doi.org/10.1007/s00253-020-10819-1.

[52] Jin W, Li T, Huo D, Qu S, Li X, Arifuzzaman M, et al. Genetic manipulation of gut microbes enables single-gene interrogation in a complex microbiome. CELL 2022;185:547. https://doi.org/10.1016/j.cell.2021.12.035.

[53] Cao X, Slavoff SA. Non-AUG start codons: expanding and regulating the small and alternative ORFeome. Exp Cell Res 2020;391:111973. https://doi.org/10.1016/j.yexcr.2020.111973.

[54] Yang G, Cozad MA, Holland DA, Zhang Y, Luesch H, Ding Y. Photosynthetic production of sunscreen shinorine using an engineered *Cyanobacterium*. ACS Synth Biol 2018;7:664–71. https://doi.org/10.1021/acssynbio.7b00397.